DALTON
FULL PAPER

Structure dependence on redox state and charge in $[Fe_4(\mu_3\text{-}S_4)(\eta\text{-}C_5H_5)_4]_m[M(mnt)_2]_n$ (M = Ni or Pt, *m*, *n* = 1 or 2)

Dena Bellamy,[a] Aristides Christofides,[a] Neil G. Connelly,*[a] Gareth R. Lewis,[a] A. Guy Orpen*[a] and Peter Thornton[b]

[a] *School of Chemistry, University of Bristol, Bristol, UK BS8 1TS. E-mail: neil.connelly@bristol.ac.uk*
[b] *Department of Chemistry, Queen Mary and Westfield College, Mile End Road, London, UK E1 4NS*

Received 2nd August 2000, Accepted 22nd September 2000
First published as an Advance Article on the web 30th October 2000

The complex salts $[Fe_4(\mu_3\text{-}S)_4(\eta\text{-}C_5H_5)_4]_m[M(mnt)_2]_n$ {M = Ni, *n* = 2, *m* = 1 **1**; *n* = 1, *m* = 1 **2** or 2 **3**: M = Pt, *n* = 2, *m* = 1 **4**; *n* = 1, *m* = 1 **5** or 2 **6**; mnt = $S_2C_2(CN)_2$} have been synthesized by stoichiometric reactions between $[NEt_4]_n[M(mnt)_2]$ (*n* = 1 or 2, M = Ni or Pt) and $[Fe_4(\mu_3\text{-}S)_4(\eta\text{-}C_5H_5)_4][PF_6]_n$ (*n* = 1 or 2); the salts **2**–**6** have been structurally characterised. The molecular structures of the $[Fe_4(\mu_3\text{-}S)_4(\eta\text{-}C_5H_5)_4]^{z+}$ (*z* = 1 or 2) cations and the $[M(mnt)_2]^{z-}$ (M = Ni or Pt, *z* = 1 or 2) anions show mean Fe · · · Fe and M–S distances characteristic of *z*. The isostructural salts $[Fe_4(\mu_3\text{-}S)_4(\eta\text{-}C_5H_5)_4]_2[M(mnt)_2]$ (M = Ni **3** or Pt **6**) comprise two monocations and one dianion; the planar anions, which form a ruffled ribbon arrangement, are interleaved by the near-spherical cations. The structure of $[Fe_4(\mu_3\text{-}S)_4(\eta\text{-}C_5H_5)_4][Pt(mnt)_2]_2$, **4**, with two monoanions and one dication, has face-to-face metal–metal pairs of $[Pt(mnt)_2]^-$ ions separated by individual $[Pt(mnt)_2]^-$ units, leading to anion layers interleaved by layers of cations. Salts **2** and **5** have very different structures. The nickel complex $[Fe_4(\mu_3\text{-}S)_4(\eta\text{-}C_5H_5)_4][Ni(mnt)_2]$ **2** comprises dications and dianions whereas the platinum complex $[Fe_4(\mu_3\text{-}S)_4(\eta\text{-}C_5H_5)_4][Pt(mnt)_2]$ **5** has monocations and monoanions. In salt **2** the dianions are well separated while in **5** the monoanions are weakly dimerised.

Introduction

Low dimensional molecular solids containing transition metal complexes have been studied extensively,[1] due to their unusual physical (optical, electrical and magnetic) properties. Our studies in this area are focused on the synthesis of crystalline solids containing redox-active cations and/or anions in order to explore the effects of the geometry and charge of the individual ions on the structural properties of the resulting salts. For example, the crystal structures of salts containing square planar $[Pt(CNMe)_4]^{2+}$ and $[M(mnt)_2]^{z-}$ {M = Pd or Pt, *z* = 1 or 2; M = Au, *z* = 1; mnt = $S_2C_2(CN)_2$} vary with the metal, M (*e.g.* Pt *vs.* Au), and with the charge and magnetic state of the anion.[2,3] Moreover, the three crystalline forms of $[Pt(CNMe)_4][M(mnt)_2]_2 \cdot solv$ (solv = $MeNO_2$, MeCN or nothing)[3] showed structure-dependent antiferromagnetism, reflecting the differing arrangements of the (*S* = 1/2) $[Pt(mnt)_2]^-$ anions within the solids.

We now describe the synthesis and structures of related salts in which *both* ions, namely $[Fe_4(\mu_3\text{-}S)_4(\eta\text{-}C_5H_5)_4]^{z+}$ (*z* = 1 or 2) and $[M(mnt)_2]^{z-}$ (M = Ni or Pt, *z* = 1 or 2), are redox-active. The various possible combinations of cubane-like (approximately spherical) cations with planar (albeit of finite thickness) anions provide the opportunity to probe the effect of the charge and redox state of the component ions on the crystal structures of the complex salts.

Results and discussion

Synthesis of complex salts

In general the new salts $[Fe_4(\mu_3\text{-}S)_4(\eta\text{-}C_5H_5)_4]_m[M(mnt)_2]_n$ {M = Ni, *n* = 2, *m* = 1 **1**; *n* = 1, *m* = 1 **2** or 2 **3**: M = Pt, *n* = 2, *m* = 1 **4**; *n* = 1, *m* = 1 **5** or 2 **6**} were synthesized by the stoichiometric reaction of $[NEt_4]_n[M(mnt)_2]$ (*n* = 1 or 2, M = Ni or Pt) with $[Fe_4(\mu_3\text{-}S)_4(\eta\text{-}C_5H_5)_4][PF_6]_n$ (*n* = 1 or 2) in either dichloromethane or acetonitrile. In each case the product usually formed directly as a pure precipitate; elemental analyses are given in Table 1. Samples suitable for X-ray crystallography were prepared by the slow diffusion together of solutions of the two reactants in a solvent in which the product was insoluble. Single crystals of **1** suitable for an X-ray structural study could not be prepared.

Table 1 Analytical and spectroscopic data for complexes **1**–**6**

Salt	Yield (%)	Elemental analyses[a] (%) C	H	N
1 $[Fe_4(\mu_3\text{-}S)_4(\eta\text{-}C_5H_5)_4][Ni(mnt)_2]_2$	87	37.1 (36.9)	2.4 (2.6)	3.6 (3.6)
2 $[Fe_4(\mu_3\text{-}S)_4(\eta\text{-}C_5H_5)_4][Ni(mnt)_2]$	60	35.2 (35.4)	2.1 (2.1)	5.7 (5.9)
3 $[Fe_4(\mu_3\text{-}S)_4(\eta\text{-}C_5H_5)_4]_2[Ni(mnt)_2]$	69	36.5 (36.9)	2.7 (2.6)	3.5 (3.6)
4 $[Fe_4(\mu_3\text{-}S)_4(\eta\text{-}C_5H_5)_4][Pt(mnt)_2]_2$	89	27.9 (27.7)	1.2 (1.3)	6.9 (7.2)
5 $[Fe_4(\mu_3\text{-}S)_4(\eta\text{-}C_5H_5)_4][Pt(mnt)_2]$	78	30.9 (30.9)	1.7 (1.9)	5.0 (5.1)
6 $[Fe_4(\mu_3\text{-}S)_4(\eta\text{-}C_5H_5)_4]_2[Pt(mnt)_2]$	58	33.6 (33.9)	2.3 (2.4)	3.2 (3.3)

[a] Calculated values in parentheses.

 DOI: 10.1039/b006262f

Crystal structure studies

Aspects of the crystal structures of the salts $[Fe_4(\mu_3\text{-}S)_4(\eta\text{-}C_5H_5)_4][Ni(mnt)_2]$ **2**, $[Fe_4(\mu_3\text{-}S)_4(\eta\text{-}C_5H_5)_4]_2[Ni(mnt)_2]$ **3**, $[Fe_4(\mu_3\text{-}S)_4(\eta\text{-}C_5H_5)_4][Pt(mnt)_2]_2$ **4**, $[Fe_4(\mu_3\text{-}S)_4(\eta\text{-}C_5H_5)_4][Pt(mnt)_2]$ **5** and $[Fe_4(\mu_3\text{-}S)_4(\eta\text{-}C_5H_5)_4]_2[Pt(mnt)_2]$ **6** are shown in Figs. 1–8; selected structural data are summarised in Tables 2 and 3.

Molecular structures of the constituent ions. The cubane-like cluster cations $[Fe_4(\mu_3\text{-}S)_4(\eta\text{-}C_5H_5)_4]^{z+}$ ($z = 1$ or 2) comprise two interpenetrating distorted tetrahedra, one of sulfur atoms and the other of iron atoms. Table 2 gives the iron–iron distances and their averages for the cations of complexes **2**–**6** as well as those in the neutral cluster $[Fe_4(\mu_3\text{-}S)_4(\eta\text{-}C_5H_5)_4]$[4,5] and other salts of its cation[6–8] and dication[9] for comparison. Although there is no significant change in the average Fe–C or Fe–S distances upon oxidation of the cluster, the Fe_4S_4 core is very flexible. The distortion of the two tetrahedra varies not only with the iron oxidation state but also with the counter anion, leading to rather variable and non-diagnostic individual Fe–Fe distances. However, the mean Fe–Fe distance is diagnostic of the oxidation state, as has been noted previously by Green and co-workers.[8] Thus, a comparison of the structures of $[Fe_4(\mu_3\text{-}S)_4(\eta\text{-}C_5H_5)_4]$[4,5] and of the cationic clusters $[Fe_4(\mu_3\text{-}S)_4(\eta\text{-}C_5H_5)_4][A]$ ($A = Br^-$,[6] $[PF_6]^-$[7] or $[Fe_4(\mu_3\text{-}S)_4(NO)_4]^-$[8]) and $[Fe_4(\mu_3\text{-}S)_4(\eta\text{-}C_5H_5)_4][PF_6]_2$[9] with those of **2**–**6** indicates the presence of monocations in **3**, **5** and **6** (mean Fe–Fe distance = 3.04–3.06 Å) and dications in **2** and **4** (mean Fe–Fe distance = 2.96–3.00 Å). The flexibility of the Fe_4S_4 core is further illustrated in the structure of **4**, which contains two formula units per crystallographic asymmetric unit. Whilst the two dications in the structure have differing sets of intramolecular Fe–Fe separations, their mean Fe–Fe distances are the same.

The metal–sulfur bond distances within the square planar anions of complexes **2**–**6** (Table 2) are consistent with those found in the crystal structures of other salts of these anions. As indicated in Table 2, d^8 M^{II}–S bonds are slightly longer than d^7 M^{III}–S bonds (by *ca.* 0.02–0.03 Å),[10] as we have also previously observed.[3] {For simplicity, *formal* oxidation states of II and III are assigned to the metal atoms of $[M(mnt)_2]^{2-}$ and $[M(mnt)_2]^-$ (M = Ni or Pt) respectively.} The M–S distances for the mono- and di-anions are therefore sufficiently different to allow the charge z of $[M(mnt)_2]^z$ ($z = -1$ or -2) to be determined from the M–S distances. Thus, the anions of **4** and **5** are assigned charges of −1, while **2**, **3** and **6** contain dianions.

The packing efficiency of these salts of $[Fe_4(\mu_3\text{-}S)_4(\eta\text{-}C_5H_5)_4]^{z+}$ can be calculated once the molecular volumes of the constituent ions have been approximated by computation of their Connolly surfaces.[11] Using a probe radius of 1.4 Å, the volumes of the mono- and di-cationic clusters were computed to vary little, with values *ca.* 370 $Å^3$ (Table 2). Similarly there are only small variations between the volumes of the anions (as given by the calculated Connolly surfaces) but the nickel complexes have marginally smaller volumes (*ca.* 215 $Å^3$) than the platinum analogues (*ca.* 224 $Å^3$).

Crystal structures of salts 2–6. An indication of the packing efficiency of the constituent ions in the crystal lattice is given by a packing coefficient, k, defined as the ratio of the molecular volume, V_{mol}, to the volume available in the particular condensed phase;[12] for crystals, $k = ZV_{mol}/V_{cell}$. The calculated packing coefficients, k, for the crystal structures of **2**–**6** therefore range from 0.70 to 0.74 (Table 2). The high values of k indicate that although of markedly different size and shape, the pseudo-spherical cubane-like cluster cations and the brick-shaped anions are packed efficiently in these crystal structures. The values of k are independent of the stoichiometry of the salt so that the different magnitude of electrostatic attraction between the ions does not apparently affect the density of packing within the crystal lattices.

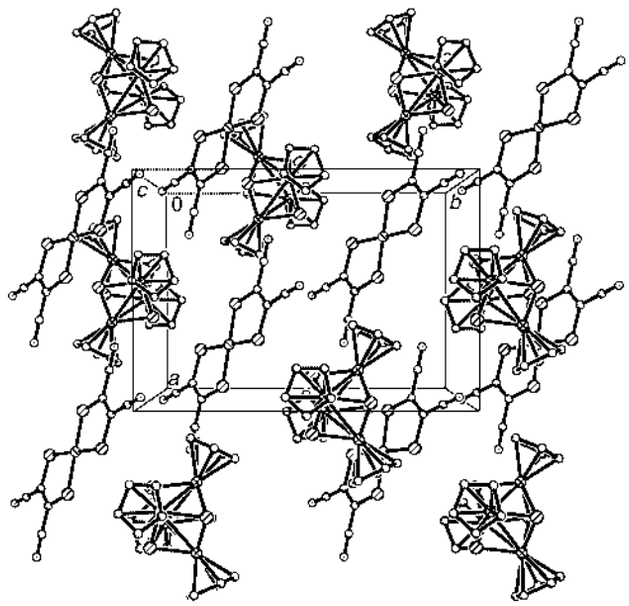

Fig. 1 The crystal structure of complex **2** as viewed along the *c* axis. Hydrogen atoms have been omitted for clarity in this and all subsequent Figures.

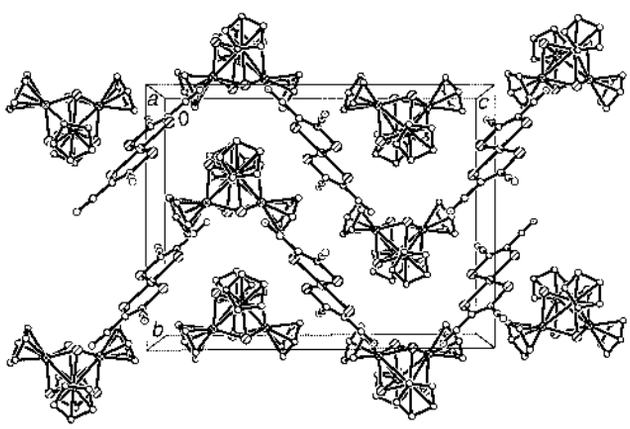

Fig. 2 The crystal structure of complex **2** as viewed along the *a* axis.

On the basis of the mean Fe–Fe and Ni–S distances noted above, the salt $[Fe_4(\mu_3\text{-}S)_4(\eta\text{-}C_5H_5)_4][Ni(mnt)_2]$ **2** may be assigned as containing $[Fe_4(\mu_3\text{-}S)_4(\eta\text{-}C_5H_5)_4]^{2+}$ dications and $[Ni(mnt)_2]^{2-}$ dianions. The assignment of a dication : dianion structure is, however, surprising not only because the platinum-containing complex **5** contains singly charged species (see below) but also on the basis of the redox potentials for the reversible couples $[Fe_4(\mu_3\text{-}S)_4(\eta\text{-}C_5H_5)_4]^{2+/+}$ ($E^{\circ\prime} = 0.43$ V) and $[M(mnt)_2]^{2-/-}$ (M = Ni, $E^{\circ\prime} = 0.17$ V; M = Pt, $E^{\circ\prime} = 0.18$ V). Thus, electron transfer between the dication and dianion, to give the monocation and monoanion, is thermodynamically favoured in solution by *ca.* 250 mV for both nickel and platinum. Presumably, the lattice energy of the dication : dianion structure provides the driving force to perturb the equilibrium in eqn. (1) to the left.

$$[Fe_4(\mu_3\text{-}S)_4(\eta\text{-}C_5H_5)_4]^{2+} + [Ni(mnt)_2]^{2-} \rightleftharpoons [Fe_4(\mu_3\text{-}S)_4(\eta\text{-}C_5H_5)_4]^{+} + [Ni(mnt)_2]^{-} \quad (1)$$

The nickel anion of complex **2** is situated at a crystallographic inversion centre, and the cluster cation on a crystallographic C_2 axis. The crystal structure of **2** contains chains of anions separated by chains of cations. The anions are arranged in a very slipped face-to-face manner (Fig. 2) with the angle of slippage (defined as the angle made by the Ni···Ni vector to the perpendicular to the NiS_4 square plane) 53.4(2)°; the

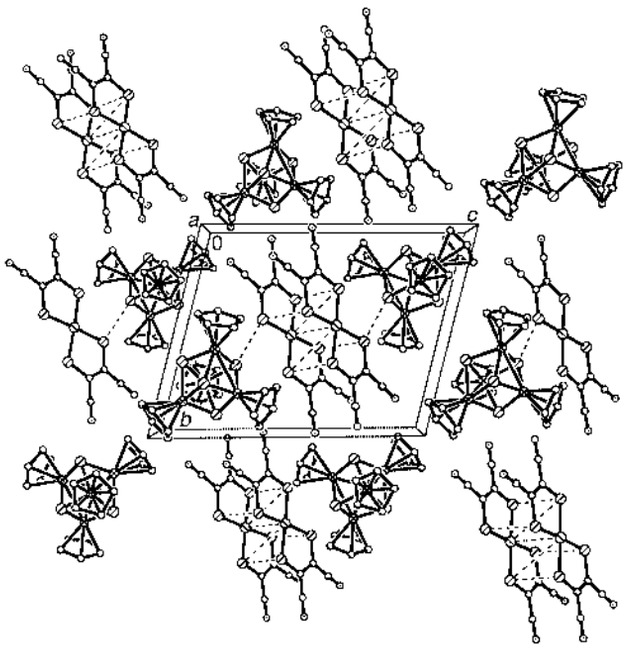

Fig. 3 The crystal structure of complex **5** as viewed along the *a* axis.

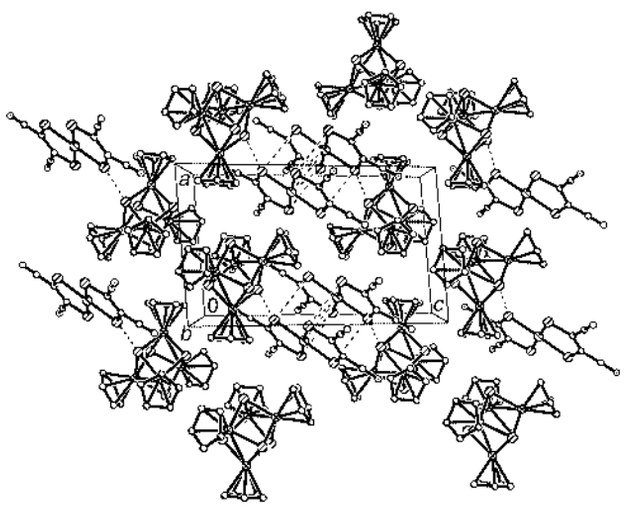

Fig. 4 The crystal structure of complex **5** as viewed along the *b* axis.

Ni · · · Ni distance is 9.284(5) Å and the planes of the $[Ni(mnt)_2]^{2-}$ anions within the chain are separated by 3.110(4) Å. The anion chains are separated by rows of $[Fe_4(\mu_3\text{-}S)_4(\eta\text{-}C_5H_5)_4]^{2+}$ cations, which are situated above and below each $[Ni(mnt)_2]^{2-}$ face (Fig. 1). The closest cation–anion contact has a N · · · H distance of 2.556(3) Å.

The Fe–Fe and Pt–S bond lengths in $[Fe_4(\mu_3\text{-}S)_4(\eta\text{-}C_5H_5)_4][Pt(mnt)_2]$ **5**, superficially an analogue of **2**, indicate instead that singly charged ions are present so that the salt is composed of monocations and monoanions. This change in charge distribution results in a markedly different structure for **5** compared with that of **2**. The slipped anion–anion arrangement of **2** is replaced by face-to-face metal–metal anion dimers in the structure of **5**. The Pt · · · Pt distance is 3.522(5) Å with an angle of slippage within the dimer of 5.9(2)°. These dimers align in a slipped chain, with an angle of slippage of 42.3(3)°, and a closest interdimer Pt · · · Pt distance of 9.119(7) Å (Fig. 3). The cluster cations are offset from the faces of the dimers, and oriented such that there are two short S · · · S contacts of 3.475(4) Å to the $[Pt(mnt)_2]^-$ anion (Fig. 4). The face-to-face dimerisation of $[Pt(mnt)_2]^-$ anions has been noted in a variety of salts.[2,3]

The salt $[Fe_4(\mu_3\text{-}S)_4(\eta\text{-}C_5H_5)_4]_2[Ni(mnt)_2]$ **3** comprises two $[Fe_4(\mu_3\text{-}S)_4(\eta\text{-}C_5H_5)_4]^+$ monocations and one $[Ni(mnt)_2]^{2-}$ dianion giving a monoclinic structure with the nickel atom located at a crystallographic inversion centre. The anions of **3** can be considered to form highly slipped face-to-face dimers, with an angle of slippage of 59.0(5)° and a Ni · · · Ni distance of 11.345(8) Å. The monocations are situated above and below the dianions, with Ni · · · H interactions of length 3.062(4) Å occupying the axial coordination sites of the nickel atom. The ions are linked by a network of weak hydrogen bonds [S · · · H 2.754(4), N · · · H 2.822(2) Å]. The structure of **3** comprises slipped stacks of anions sandwiched between two cations (Fig. 6). The direction of the stacks in the structure alternates, and when viewed as a projection down the *c* axis an overall ribbon-like arrangement is observed (Fig. 5).

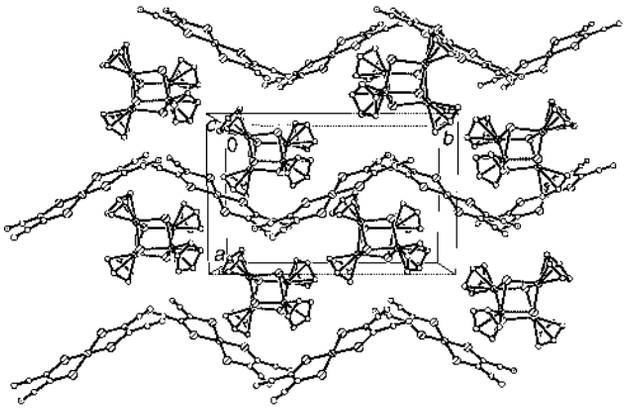

Fig. 5 The crystal structure of complex **3** as viewed along the *c* axis.

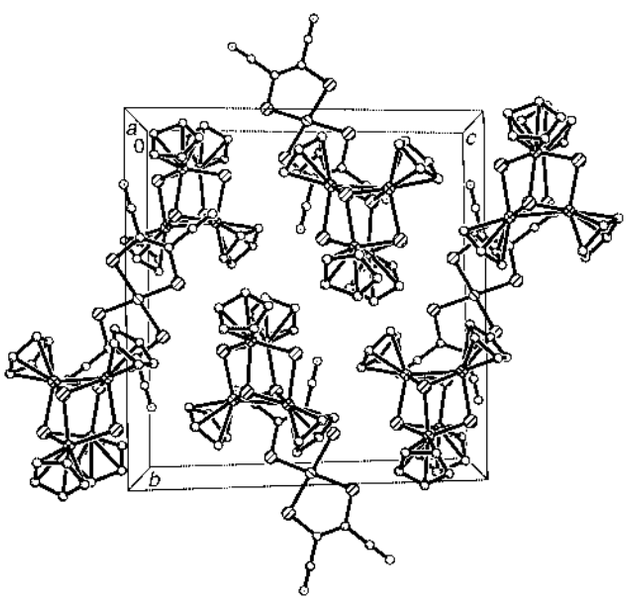

Fig. 6 The crystal structure of complex **3** as viewed along the *a* axis.

As seen in Table 2, $[Fe_4(\mu_3\text{-}S)_4(\eta\text{-}C_5H_5)_4]_2[Pt(mnt)_2]$ **6** is isostructural with **3**; small differences in the intermolecular distances may be attributed to the larger size of $[Pt(mnt)_2]^-$ compared with that of $[Ni(mnt)_2]^-$. The axial Pt · · · H distance is 3.082(4) Å, the closest intermolecular S · · · H distance 2.693(3) Å, and the cation · · · anion N · · · H bond 2.806(3) Å. The angle of slippage of the anions is 55.2(6)°, with intralayer Pt · · · Pt distances of 11.304(7) Å and interlayer Pt · · · Pt distances of 10.594(6) Å.

The combination of two $[Pt(mnt)_2]^-$ anions with one dication yields $[Fe_4(\mu_3\text{-}S)_4(\eta\text{-}C_5H_5)_4][Pt(mnt)_2]_2$ **4**, which has a markedly different structure from those described above (Figs. 7 and 8). There are two types of anion environment. First, there are face-to-face metal–metal dimers with a Pt · · · Pt distance of 3.524(4) Å and an angle of slippage of 6.5(2)°. These dimers, denoted Pt_{dimer}, are separated by single $[Pt(mnt)_2]^-$ ions

Table 2 Selected structural data for **2**–**6** and related complexes

Complex	Fe–Fe distances/Å	Mean Fe–Fe/Å	M–S[a]/Å	MS_4 deviation[b]/Å	Volume[c]/Å^3 cation	Volume[c]/Å^3 anion	Packing coefficient,[d] k
$[Fe_4(\mu_3\text{-}S)_4(\eta\text{-}C_5H_5)_4]$	1 × 2.62, 1 × 2.64, 4 × 3.37[e]	3.13	—	—	—	—	
	2 × 2.65, 4 × 3.36[f]	3.12					
$[Fe_4(\mu_3\text{-}S)_4(\eta\text{-}C_5H_5)_4]Br$[g]	2 × 2.65, 2 × 3.19, 2 × 3.32	3.05	—	—	—	—	—
$[Fe_4(\mu_3\text{-}S)_4(\eta\text{-}C_5H_5)_4][PF_6]$[h]	2 × 2.66, 2 × 3.19, 2 × 3.30[i]	3.05	—	—	—	—	—
	2 × 2.63, 2 × 3.21, 2 × 3.30[j]	3.05					
$[Fe_4(\mu_3\text{-}S)_4(\eta\text{-}C_5H_5)_4][Fe_4S_4(NO)_4]$[k]	2 × 2.66, 1 × 3.01, 3 × 3.32	3.05	—	—	—	—	—
$[Fe_4(\mu_3\text{-}S)_4(\eta\text{-}C_5H_5)_4][PF_6]_2$[l]	4 × 2.83, 2 × 3.25	3.00	—	—	—	—	—
2	2 × 2.66, 2 × 2.97, 2 × 3.27	2.97	2.173(3)	0.000	378.9	214.3	0.73
3	2 × 2.65, 1 × 3.01, 3 × 3.34	3.06	2.170(3)	0.000	365.2	217.4	0.70
4[m]	2 × 2.65, 1 × 2.90, 1 × 3.08, 2 × 3.26;	2.97;	2.269(4)	0.065, 0.064	370.4	223.9	0.74
	3 × 2.65, 3 × 3.27	2.96		0.018, 0.006			
5	2 × 2.65, 1 × 3.00, 3 × 3.32	3.04	2.270(8)	0.008	371.1	223.3	0.72
6	2 × 2.66, 1 × 2.99, 3 × 3.34	3.06	2.294(3)	0.000	364.2	225.1	0.72

[a] The mean M–S values for the anions. Literature values: average Ni–S from 15 examples of $[Ni(mnt)_2]^-$ = 2.144(4) Å; average Ni–S from 20 examples of $[Ni(mnt)_2]^{2-}$ = 2.173(5) Å; average Pt–S from 18 examples of $[Pt(mnt)_2]^-$ = 2.264(4) Å; average Pt–S from 4 examples of $[Pt(mnt)_2]^{2-}$ = 2.288(5) Å; from the Cambridge Structural database.[10] [b] The deviation of M from the plane of the 4 S atoms of the two mnt ligands. [c] Calculated as the volume mapped out by the Connolly surface for the constituent ions using the CERIUS^2 molecular modelling software.[16] [d] $k = ZV_{mol}/V_{cell}$,[12] where V_{mol} is the sum of the volumes of the constituent ions of the salt, as given by the Connolly surfaces. [e] Orthorhombic form, from ref. 4. [f] Monoclinic form, from ref. 5. [g] From reference 6. [h] From reference 7. [i] Monoclinic form. [j] Tetragonal form. [k] From reference 8. [l] From reference 9. [m] Two cations in asymmetric unit.

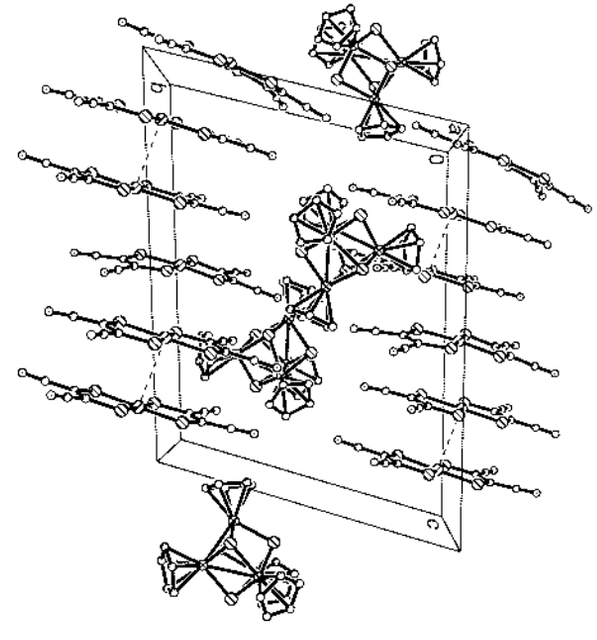

Fig. 7 The crystal structure of complex **4** as viewed along the *c* axis.

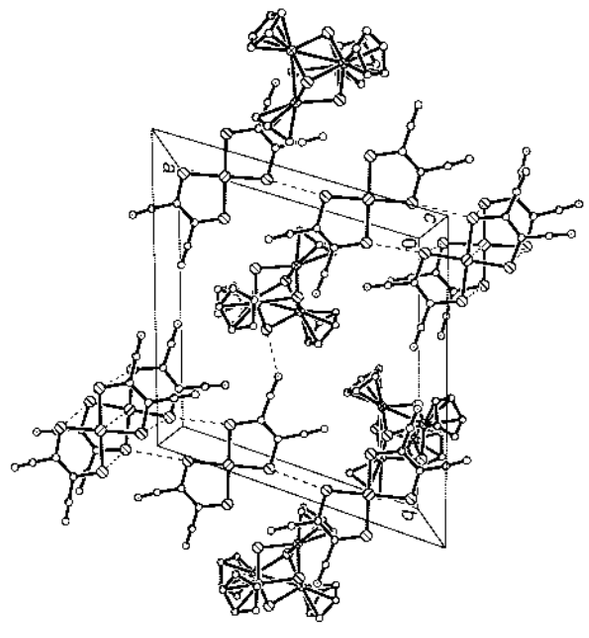

Fig. 8 The crystal structure of complex **4** as viewed along the *a* axis.

(denoted Pt_{lone}), slipped with respect to the dimer by 22.7°, giving a closest $Pt_{dimer} \cdots Pt_{lone}$ distance of 4.858(6) Å. Thus, the lone monoanions are offset from the dimers which align above each other to form a column in which the Pt···Pt distance is 7.809(6) Å (Fig. 7). The dications are situated between the anionic layers, and can also be considered to form a column. There are many hydrogen bonds (at less than 2.8 Å) between the $\eta\text{-}C_5H_5$ rings and the nitrogen atoms of the anions; the shortest N···H distance is 2.456(4) Å. The cations and anions are further linked by nitrogen–sulfur van der Waals interactions at a distance of 3.184(4) Å (Fig. 8).

Conclusion

The synthesis of the salts **2**–**6** has allowed an investigation of the effect of the charge of the constituent ions on structure. Changing the oxidation state of the metal atom of the anionic dithiolene complex has a significant effect: **2** has a markedly different crystal structure from that of **5**, whilst **3** and **6** are isostructural. In **2**, **3** and **6**, the anionic dithiolene complexes contain d^8 metal atoms. In contrast, the metal atoms of **5** have a formal d^7 electronic configuration.

Table 3 Crystal and other stuctural data for complexes **2**–**6**[a]

	2	**3**	**4**	**5**	**6**
Empirical formula	$C_{28}H_{20}Fe_4N_4NiS_8$	$C_{48}H_{40}Fe_8N_4NiS_{12}$	$C_{36}H_{20}Fe_4N_8Pt_2S_{12}$	$C_{28}H_{20}Fe_4N_4PtS_8$	$C_{48}H_{40}Fe_8N_4PtS_{12}$
M	951.07	1563.07	1562.90	1087.45	1699.68
Crystal colour, habit	Black cubes	Black diamonds	Black plates	Black diamonds	Black diamonds
Crystal system	Monoclinic	Monoclinic	Triclinic	Triclinic	Monoclinic
Space group (no.)	$C2/c$ (15)	$P2_1/c$ (14)	$P\bar{1}$ (2)	$P\bar{1}$ (2)	$P2_1/c$ (14)
a/Å	10.6970(10)	10.6645(11)	15.4336(11)	9.1195(10)	10.5944(10)
b/Å	15.1764(12)	16.224(2)	15.681(2)	12.193(2)	16.3005(15)
c/Å	20.0577(13)	15.863(2)	20.781(3)	15.364(3)	15.6650(15)
α/°			99.398(9)	104.153(10)	
β/°	93.224(8)	100.836(10)	109.254(14)	94.414(8)	100.977(15)
γ/°			103.937(13)	90.920(6)	
V/Å^3	3251.06(4)	2695.7(5)	4443.6(7)	1650.52(53)	2655.8(6)
Z	4	2	4	2	2
μ/mm^{-1}	2.854	2.933	8.149	6.474	5.253
Reflections collected	10179	7640	21349	7549	12487
Independent reflections	3686	6171	15053	5585	4657
R_{int}	0.0298	0.0328	0.0330	0.0383	0.0473
Final R indices: $R1$ [$I > 2\sigma(I)$]	0.0270	0.0448	0.0402	0.0308	0.0232
$wR2$	0.0542	0.1311	0.0778	0.0817	0.0573

[a] Diffraction measurements were made at 173 K in all cases.

Experimental

The complexes described were prepared under an atmosphere of dry nitrogen using dried, distilled and deoxygenated solvents, and are air-stable in the solid state and insoluble in all common organic solvents. The complexes $[Fe_4(\mu_3\text{-}S)_4(\eta\text{-}C_5H_5)_4][PF_6]_n$ ($n = 0$,[5] 1[6] or 2[9]) and $[NEt_4]_n[M(mnt)_2]$ (M = Ni or Pt, $n = 2$[13] or 1[14]) were prepared by published methods. Where an H-tube was used for crystal growth, solutions of the two reactants were placed in the separate legs of the apparatus. The horizontal crossbar was then slowly filled with the same solvent, and the tube sealed. Slow diffusion together of the two solutions led to the formation of crystals. The potentials for the couples $[Fe_4(\mu_3\text{-}S)_4(\eta\text{-}C_5H_5)_4]^{2+/+}$ and $[M(mnt)_2]^{2-/-}$ (M = Ni or Pt) were determined in CH_2Cl_2 by cyclic voltammetry using methods previously described,[15] with either $[Fe(\eta\text{-}C_5H_5)_2]$ (for the anions) or $[Fe(\eta\text{-}C_5Me_5)_2]$ (for the cation) added to the test solutions as an internal calibrant. (On this scale, the one-electron oxidation of $[Fe(\eta\text{-}C_5H_5)_2]$ occurs at 0.47 V.) Crystal structures were analysed and Connolly surfaces computed using the CERIUS[2] software package.[16] Microanalyses were carried out by the staff of the Microanalytical Service of the School of Chemistry, University of Bristol.

Preparations

$[Fe_4(\mu_3\text{-}S)_4(\eta\text{-}C_5H_5)_4][Ni(mnt)_2]_2$ 1. To a solution of $[NEt_4][Ni(mnt)_2]$ (94 mg, 0.20 mmol) in CH_2Cl_2 (10 cm^3) was added solid $[Fe_4(\mu_3\text{-}S)_4(\eta\text{-}C_5H_5)_4][PF_6]_2$ (92 mg, 0.10 mmol). After 5 d the mother liquors were removed and the black solid was washed with CH_2Cl_2 before drying *in vacuo*, yield 113 mg (87%).

$[Fe_4(\mu_3\text{-}S)_4(\eta\text{-}C_5H_5)_4][Ni(mnt)_2]$ 2. *(a) Powder.* To a solution of $[Fe_4(\mu_3\text{-}S)_4(\eta\text{-}C_5H_5)_4][PF_6]$ (40 mg, 0.053 mmol) in CH_2Cl_2 (10 cm^3) was added solid $[NEt_4][Ni(mnt)_2]$ (25 mg, 0.053 mmol). After 1 h, addition of *n*-hexane (10 cm^3) induced the formation of a black solid which was collected and dried *in vacuo*, yield 25 mg (60%).

(b) Crystals. In an H-tube, a solution of $[NEt_4][Ni(mnt)_2]$ (120 mg, 0.264 mmol) in MeCN (20 cm^3) was allowed to diffuse slowly (*ca.* 6 weeks) into a solution of $[Fe_4(\mu_3\text{-}S)_4(\eta\text{-}C_5H_5)_4][PF_6]$ (200 mg, 0.264 mmol) in MeCN (25 cm^3). The black crystals were collected, washed with MeCN and dried *in vacuo*, yield 156 mg (62%).

$[Fe_4(\mu_3\text{-}S)_4(\eta\text{-}C_5H_5)_4]_2[Ni(mnt)_2]$ 3. In an H-tube, a solution of $[NEt_4]_2[Ni(mnt)_2]$ (58 mg, 0.10 mmol) in MeCN (20 cm^3) was allowed to diffuse slowly (*ca.* 2 weeks) into a solution of $[Fe_4(\mu_3\text{-}S)_4(\eta\text{-}C_5H_5)_4][PF_6]$ (150 mg, 0.20 mmol) in MeCN (20 cm^3). The resulting black crystals were collected, washed with MeCN and dried *in vacuo*, yield 106 mg (69%).

$[Fe_4(\mu_3\text{-}S)_4(\eta\text{-}C_5H_5)_4][Pt(mnt)_2]_2$ 4. *(a) Powder.* To a solution of $[NEt_4][Pt(mnt)_2]$ (121 mg, 0.20 mmol) in CH_2Cl_2 (10 cm^3) was added $[Fe_4(\mu_3\text{-}S)_4(\eta\text{-}C_5H_5)_4][PF_6]_2$ (90 mg, 0.10 mmol). After stirring the mixture for 7 d the black precipitate was collected, washed with CH_2Cl_2 and dried *in vacuo*, yield 139 mg (89%).

(b) Crystals. In an H-tube, a solution of $[NEt_4][Pt(mnt)_2]$ (125 mg, 0.21 mmol) in MeCN (22 cm^3) was allowed to diffuse slowly (*ca.* 4 weeks) into a solution of $[Fe_4(\mu_3\text{-}S)_4(\eta\text{-}C_5H_5)_4][PF_6]_2$ (90 mg, 0.10 mmol) in MeCN (23 cm^3). The black crystals were collected, washed with MeCN and dried *in vacuo*, yield 88 mg (54%).

$[Fe_4(\mu_3\text{-}S)_4(\eta\text{-}C_5H_5)_4][Pt(mnt)_2]$ 5. *(a) Powder.* Addition of a solution of $[Fe_4(\mu_3\text{-}S)_4(\eta\text{-}C_5H_5)_4][PF_6]$ (76 mg, 0.10 mmol) in CH_2Cl_2 (10 cm^3) to a solution of $[NEt_4][Pt(mnt)_2]$ (61 mg, 0.10 mmol) in CH_2Cl_2 (10 cm^3) immediately gave a black precipitate which was collected, washed with CH_2Cl_2 and dried *in vacuo*, yield 78 mg (78%).

(b) Crystals. In an H-tube, a solution of $[NEt_4][Pt(mnt)_2]$ (155 mg, 0.261 mmol) in CH_2Cl_2 (25 cm^3) was allowed to diffuse slowly (*ca.* 4 weeks) into a solution of $[Fe_4(\mu_3\text{-}S)_4(\eta\text{-}C_5H_5)_4][PF_6]$ (199 mg, 0.262 mmol) in CH_2Cl_2 (25 cm^3). The black crystals were collected, washed with CH_2Cl_2 and dried *in vacuo*, yield 141 mg (50%).

$[Fe_4(\mu_3\text{-}S)_4(\eta\text{-}C_5H_5)_4]_2[Pt(mnt)_2]$ 6. *(a) Powder.* To a solution of $[Fe_4(\mu_3\text{-}S)_4(\eta\text{-}C_5H_5)_4][PF_6]$ (76 mg, 0.10 mmol) in CH_2Cl_2 (30 cm^3) was added a solution of $[NEt_4]_2[Pt(mnt)_2]$ (37 mg, 0.05 mmol) in CH_2Cl_2 (40 cm^3). After 5 d the black microcrystalline solid was collected, washed with CH_2Cl_2 and dried *in vacuo*, yield 50 mg (58%).

(b) Crystals. In an H-tube, a solution of $[NEt_4]_2[Pt(mnt)_2]$ (72 mg, 0.10 mmol) in CH_2Cl_2 (15 cm^3) was allowed to diffuse slowly (*ca.* 4 weeks) into a solution of $[Fe_4(\mu_3\text{-}S)_4(\eta\text{-}C_5H_5)_4][PF_6]$ (150 mg, 0.20 mmol) in CH_2Cl_2 (15 cm^3). The black crystals were collected, washed with CH_2Cl_2 and dried *in vacuo*, yield 104 mg (50%).

Crystallography

Crystal data and other details of the structure analyses are presented in Table 3.

CCDC reference number 186/2191.

See http://www.rsc.org/suppdata/dt/b0/b006262f/ for crystallographic files in .cif format.

Acknowledgements

We thank the EPSRC and the CCDC for research studentships (to G. R. L. and D. B. respectively).

References

1 See, for example, *Inorganic Materials*, 2nd edn., eds. D. W. Bruce and D. O'Hare, John Wiley & Sons, New York, 1996; *Extended Linear Chain Compounds*, ed. J. S. Miller, Plenum Press, New York, 1992; J. S. Miller and A. J. Epstein, *Prog. Inorg. Chem.*, 1976, **20**, 1.

2 N. G. Connelly, J. G. Crossley, A. G. Orpen and H. Salter, *J. Chem. Soc.*, *Chem. Commun.*, 1992, 1564.

3 H. Bois, N. G. Connelly, J. G. Crossley, J.-C. Guillorit, G. R. Lewis, A. G. Orpen and P. Thornton, *J. Chem. Soc.*, *Dalton Trans.*, 1998, 2833.

4 R. A. Schunn, C. J. Fritchie, Jr. and C. T. Prewitt, *Inorg. Chem.*, 1966, **5**, 892.

5 C. H. Wei, G. R. Wilkes, P. M. Treichel and L. F. Dahl, *Inorg. Chem.*, 1966, **5**, 900.

6 T. Toan, W. P. Fehlhammer and L. F. Dahl, *J. Am. Chem. Soc.*, 1977, **99**, 402.

7 M. Shimoi, A. Satoh and H. Ogino, *Bull. Chem. Soc. Jpn.*, 1991, **64**, 11.

8 P. Baird, J. A. Bandy, M. L. H. Green, A. Hamnett, E. Marseglia, D. S. Obertelli, K. Prout and J. Qin, *J. Chem. Soc.*, *Dalton Trans.*, 1991, 2377.

9 T. Toan, B. K. Teo, J. A. Ferguson, T. J. Meyer and L. F. Dahl, *J. Am. Chem. Soc.*, 1977, **99**, 408.

10 F. H. Allen, J. E. Davies, J. J. Galloy, O. Johnson, O. Kennard, C. F. Macrae, E. M. Mitchell, G. F. Mitchell, J. M. Smith and D. G. Watson, *J. Chem. Inf. Comput. Sci.*, 1991, **31**, 187; F. H. Allen and O. Kennard, *Chem. Des. Autom. News*, 1993, **8**, 1, 31.

11 M. L. Connolly, *Science*, 1983, **221**, 709; M. L. Connolly, *J. Am. Chem. Soc.*, 1985, **107**, 1118.

12 A. I. Kitaigorodskii, *Molecular Crystals and Molecules*, Academic Press, New York, 1973.

13 J. F. Weiher, L. R. Melby and R. E. Benson, *J. Am. Chem. Soc.*, 1964, **86**, 4329.

14 A. Davison, N. Edelstein, R. H. Holm and A. H. Maki, *Inorg. Chem.*, 1963, **2**, 1227.

15 N. C. Brown, G. B. Carpenter, N. G. Connelly, J. G. Crossley, A. Martin, A. G. Orpen, A. L. Rieger, P. H. Rieger and G. H. Worth, *J. Chem. Soc.*, *Dalton Trans.*, 1996, 3977.

16 CERIUS^2, Molecular Modelling Software, MSI/Biosym Inc., Cambridge, 1998, version 3.5.